

# An adaptive approximate Bayesian computation MCMC with Global-Local proposals

Xuefei Cao<sup>1</sup>, Shijia Wang<sup>2\*</sup> and Yongdao Zhou<sup>1\*</sup>

<sup>1</sup>NITFID, School of Statistics and Data Science, Nankai University, China

<sup>2</sup>Institute of Mathematical Sciences, ShanghaiTech University, China

December 23, 2024

## Abstract

In this paper, we address the challenge of Markov Chain Monte Carlo (MCMC) algorithms within the Approximate Bayesian Computation (ABC) framework, which often get trapped in local optima due to their inherent local exploration mechanism. We propose a novel Global-Local ABC-MCMC algorithm that combines the “exploration” capabilities of global proposals with the “exploitation” finesse of local proposals. By integrating iterative importance resampling into the likelihood-free framework, we establish an effective global proposal distribution. We select the optimum mixture of global and local moves based on a unit cost version of expected squared jumped distance via sequential optimization. Furthermore, we propose two adaptive schemes: The first involves a normalizing flow-based probabilistic distribution learning model to iteratively improve the proposal for importance sampling, and the second focuses on optimizing the efficiency of the local sampler by utilizing Langevin dynamics and common random numbers. We numerically demonstrate that our method improves sampling efficiency and achieve more reliable convergence for complex posteriors. A software package implementing this method is available at <https://github.com/caofff/GL-ABC-MCMC>.

*Keywords:* Approximate Bayesian computation, common random numbers, iterative sampling importance resampling, normalizing flow, sequential optimization.

## 1 Introduction

Traditional Bayesian inference typically relies on the assumption that the likelihood functions of statistical models are estimable. However, for many complex applications, these likelihood

---

\*Address correspondence to: Dr. Shijia Wang ([wangshj1@shanghaitech.edu.cn](mailto:wangshj1@shanghaitech.edu.cn)) and Dr. Yongdao Zhou ([ydzhou@nankai.edu.cn](mailto:ydzhou@nankai.edu.cn)).

functions either lack explicit expressions or are difficult to estimate numerically. *Approximate Bayesian computation* (ABC) (Pritchard et al., 1999; Beaumont et al., 2002) is a likelihood-free inference method based on simulations. It only requires simulating synthetic data from the model without evaluating the likelihood function. Rejection ABC (Tavaré et al., 1997; Pritchard et al., 1999) is the simplest and most intuitive version of ABC algorithms, which involves repeatedly drawing parameter samples  $\theta$  independently from prior  $\pi$ , simulating synthetic data  $\mathbf{x}$  for each sample of  $\theta$ , and rejecting the parameter  $\theta$  if the discrepancy  $\mathfrak{D}(\mathbf{x}, \mathbf{y})$  between the observed data  $\mathbf{y}$  and the simulated data  $\mathbf{x}$  exceeds a pre-specified tolerance threshold  $\varepsilon$ . In practice, sampling parameters from a prior distribution can be inefficient, especially in high dimensional cases, as most of samples drawn from the prior distribution fall into the low posterior regions, resulting very high rejection rates. Consequently, accepting one sample may require thousands or even millions of draws.

Marjoram et al. (2003) introduce an ABC *Markov chain Monte Carlo* (MCMC) algorithm to approximate the posterior distribution. Proposal distributions are typically chosen to generate local moves that depend on the last state of the chain to ensure an admissible acceptance rate. Theoretically, a small tolerance value  $\varepsilon$  leads to a good posterior approximation. However, designing an efficient proposal to explore the parameter space, especially in the case of high dimensional multimodal posterior distributions, poses a significant challenge. Wegmann et al. (2009) enhanced the performance of ABC-MCMC by relaxing the tolerance, incorporating subsampling, and applying regression adjustments to the MCMC output. Sisson et al. (2007); Del Moral et al. (2012) integrated ABC-MCMC algorithms into the SMC framework (Del Moral et al., 2006). The sequence of intermediate target distributions is defined by ABC posteriors with a series of tolerance parameters. Del Moral et al. (2012) adaptively determined this sequence by managing the divergence of particles. Clarté et al. (2020); Rodrigues et al. (2020) proposed Gibbs version of the ABC approaches that focuses on lower-dimensional conditional distributions. *Hamiltonian Monte Carlo* (HMC) (Duane et al., 1987; Neal et al., 2011) employs Hamiltonian dynamics to propose candidate parameters, efficiently avoiding the random walk behavior that can impede the mixing of proposals in high-dimensional spaces. (Meeds et al., 2015) explored the application of HMC to ABC and proposed using *completely random numbers* (CRNs) to improve the stability of gradient estimates to improve Hamiltonian dynamic.

However, for a high dimensional multimodal posterior distribution, all local samplers mix poorly because the exploration is inherently slow, and switching between isolated modes can be extremely rare. Independent proposals can generate more global updates to transfer particles between modes, but they are difficult to design. A poor designed independent sampler in MCMC results in an inefficient random walk, causing the algorithm to converge slowly. For likelihood-based Bayesian inference, [Samsonov et al. \(2022\)](#) improved an Explore-Exploit MCMC strategy that couples a local move and a global move in each iteration. [Gabrié et al. \(2022\)](#) performed a global move after a fixed number of local moves during MCMC iterations. Moreover, normalizing flows ([Rezende and Mohamed, 2015](#); [Papamakarios et al., 2021](#)) are used to improve the exploration capabilities of MCMC independent proposals.

In this paper, we propose a novel approach that combines the advantages of global MCMC proposal and local MCMC proposal for challenging posterior distribution within the likelihood-free framework. First, we introduce a likelihood-free *iterative-sampling importance resampling* (i-SIR) approach to construct an efficient global kernel for ABC-MCMC. We demonstrate that the ABC-i-SIR algorithm can be interpreted as a systematic-scan two-stage Gibbs sampler and prove the uniform geometric ergodicity of the ABC-i-SIR Markov kernel. Furthermore, we also establish the V-geometric ergodicity of the combination of the ABC-i-SIR Markov kernel and the local Markov kernel, and thus show that under certain conditions, the mixing rate of the Global-Local Markov Kernel is significantly better than that of the local Markov kernel. Second, we propose a sequential optimization approach based on a unit cost version of expected square jump distance (cESJD) criterion to select the hyper-parameters of Global-Local ABC-MCMC (GL-ABC-MCMC), such as the batch size of ABC-i-SIR and the mixture proportion of global and local moves. Third, we develop two adaptive schemes to enhance the efficiency of GL-ABC-MCMC by automatically constructing the local and global proposal distributions. The first scheme improves the importance proposal distribution of ABC-i-SIR using normalizing flows during the iterations of the Markov chain. The second scheme applies the Metropolis-adjusted Langevin algorithm to ABC, and utilizes common random numbers to enhance the estimate of the gradient of the log-likelihood. Our numerical experiments indicate that the proposed method can mix faster than existing methods.

The rest of paper is organized as follows. Section 2 presents our GL-ABC-MCMC, including

ABC-i-SIR, the sequential optimization of hyper-parameters and the theoretical properties. Section 3 introduces two adaptive schemes for improving the global and local proposal distributions. Sections 4 and 5 demonstrate the effectiveness of our method through synthetic examples studies and two real model analysis. Section 6 provides the conclusion, and all proofs of the theoretical results are deferred to the Supplement.

## 2 An ABC-MCMC with global and local proposals

### 2.1 A review of ABC-MCMC

We consider a given observed data set  $\mathbf{y} \in \mathbb{Y}$ , which is realized from a parametric model  $\{P_{\theta_0} : \theta_0 \in \Theta \subset \mathbb{R}^p\}$ . Assume that for each  $\theta \in \Theta$ ,  $P_{\theta}$  admits a density  $p(\cdot | \theta)$  that cannot be directly evaluated but can be sampled from. The ABC posterior can be achieved by augmenting the target posterior from  $\pi_{\varepsilon}(\theta | \mathbf{y})$  to

$$\pi_{\varepsilon}(\theta, \mathbf{x} | \mathbf{y}) = \frac{\pi(\theta)p(\mathbf{x} | \theta)K_{\varepsilon}(\mathbf{x}, \mathbf{y})}{\iint \pi(\theta)p(\mathbf{x} | \theta)K_{\varepsilon}(\mathbf{x}, \mathbf{y})d\mathbf{x}d\theta},$$

where  $\mathbf{x}$  denotes synthetic data simulated from  $p(\cdot | \theta)$ ,  $K_{\varepsilon}(\cdot, \cdot)$  is a kernel function and the threshold  $\varepsilon$  plays a role of bandwidth. The marginal posterior distribution  $\pi_{\varepsilon}(\theta | \mathbf{y})$  can be evaluated by integrating out the auxiliary data set  $\mathbf{x}$  from  $\pi_{\varepsilon}(\theta, \mathbf{x} | \mathbf{y})$ . The choice of threshold  $\varepsilon$  is a trade-off between accuracy and computational speed. A smaller value of threshold can lead to more accurate ABC posterior, but with higher computational cost. When the threshold value  $\varepsilon$  approaches to zero,  $\pi_{\varepsilon}(\mathbf{y} | \theta)$  converges to the exact Bayesian posterior  $\pi(\mathbf{y} | \theta)$ .

To sample from high-dimensional posterior space, rejection ABC is not efficient since there is often a significant mismatch between the prior distribution and the posterior. In some cases, generating millions of synthetic data sets may be required to obtain a few accepted samples. The ABC-MCMC approach is a good alternative to rejection ABC for likelihood-free inference. It uses local moves for proposing parameters, and is thus more efficient. The idea for MCMC is to construct a Markov chain whose probability density converges to the stationary distribution  $\pi_{\varepsilon}(\theta, \mathbf{x} | \mathbf{y})$ , with the marginal distribution being  $\pi_{\varepsilon}(\theta | \mathbf{y})$ . We introduce a proposal distribution  $q(\theta^* | \theta)$  and a function  $\alpha$  that satisfies

$$\pi_{\varepsilon}(\theta, \mathbf{x} | \mathbf{y})q(\theta^* | \theta)p(\mathbf{x}^* | \theta^*)\alpha[(\theta, \mathbf{x}), (\theta^*, \mathbf{x}^*)] = \pi_{\varepsilon}(\theta^*, \mathbf{x}^* | \mathbf{y})q(\theta | \theta^*)p(\mathbf{x} | \theta)\alpha[(\theta^*, \mathbf{x}^*), (\theta, \mathbf{x})],$$

where

$$\alpha [(\boldsymbol{\theta}, \mathbf{x}), (\boldsymbol{\theta}^*, \mathbf{x}^*)] = \min \left\{ 1, \frac{\pi(\boldsymbol{\theta}^*) K_\varepsilon(\mathbf{x}^*, \mathbf{y}) q(\boldsymbol{\theta} | \boldsymbol{\theta}^*)}{\pi(\boldsymbol{\theta}) K_\varepsilon(\mathbf{x}, \mathbf{y}) q(\boldsymbol{\theta}^* | \boldsymbol{\theta})} \right\}. \quad (2.1)$$

At  $(t + 1)$ -th MCMC iteration, we repeat the following procedure.

- (i) Sample  $\boldsymbol{\theta}^*$  from  $q(\cdot | \boldsymbol{\theta}_t)$ .
- (ii) Generate synthetic data  $\mathbf{x}^*$  from  $P_{\boldsymbol{\theta}^*}$ .
- (iii) Accept  $(\boldsymbol{\theta}_{t+1}, \mathbf{x}_{t+1}) = (\boldsymbol{\theta}^*, \mathbf{x}^*)$  with probability  $\alpha [(\boldsymbol{\theta}_t, \mathbf{x}_t), (\boldsymbol{\theta}^*, \mathbf{x}^*)]$ ; otherwise, set  $(\boldsymbol{\theta}_{t+1}, \mathbf{x}_{t+1}) = (\boldsymbol{\theta}_t, \mathbf{x}_t)$ .

## 2.2 An ABC-MCMC with global and local proposals

The exploration of the standard ABC-MCMC introduced in Section 2.1 is constrained to a small region around the current state. This often results in poor mixing, as particles can become trapped in some local regions, especially for multi-modal ABC posteriors. Therefore, it is necessary to design more global updates to improve the exploration ability of MCMC, helping samples move across different modes more frequently. However, globally proposing each parameter may not adequately capture the dependencies and correlations between parameters, making it challenging to explore the space effectively. By integrating both local and global proposals, the algorithm can combine the strengths of both approaches, achieving an optimal balance that allows for a detailed examination of local regions while ensuring a more comprehensive exploration of the entire parameter space.

We implement the Global-Local ABC-MCMC algorithm by alternating between local and global sampling. Specifically, we perform global sampling with probability  $\gamma$  and local sampling with probability  $1 - \gamma$  at each iteration. The transition kernel of the Global-Local ABC-MCMC is defined as:

$$k((\boldsymbol{\theta}, \mathbf{x}), (\boldsymbol{\theta}^*, \mathbf{x}^*)) = \gamma k_g((\boldsymbol{\theta}, \mathbf{x}), (\boldsymbol{\theta}^*, \mathbf{x}^*)) + (1 - \gamma) k_l((\boldsymbol{\theta}, \mathbf{x}), (\boldsymbol{\theta}^*, \mathbf{x}^*)), \quad (2.2)$$

where  $k_l$  is a local ABC-MCMC kernel, and  $k_g$  is a global ABC-MCMC kernel. This formulation provides flexibility in the explore-exploit strategy by incorporating both local and global perspectives. The parameter  $\gamma$  controls the trade-off between exploitation and exploration. When  $\gamma = 0$ , the Global-Local ABC-MCMC algorithm degenerates to the standard ABC-MCMC; otherwise, when  $\gamma = 1$ , it only utilizes a global proposal.

### 2.3 The global proposal: iteration sampling importance resample

One straightforward approach is to use a proposal distribution  $q(\cdot)$  that is independent of the previous state, serving as a global proposal. This can facilitate more frequent transitions between modes. However, with such an independent proposal, the MH acceptance probability  $\alpha[(\boldsymbol{\theta}, \mathbf{x}), (\boldsymbol{\theta}^*, \mathbf{x}^*)] = \min \left\{ 1, \frac{\pi(\boldsymbol{\theta}^*)K_\varepsilon(\mathbf{x}^*, \mathbf{y})q(\boldsymbol{\theta})}{\pi(\boldsymbol{\theta})K_\varepsilon(\mathbf{x}, \mathbf{y})q(\boldsymbol{\theta}^*)} \right\}$  tends to be very low if  $q(\cdot)$  diverges significantly from the ABC posterior. This presents challenges for the global exploration capabilities of GL-ABC-MCMC, particularly in high-dimensional spaces. Therefore, it is essential for the global proposal to be as close to the ABC posterior as possible. However, inferring this proposal is nearly as complex as inferring the ABC posterior itself. In response to this challenge, we propose a flexible approach to obtain an efficient global proposal.

*Sampling Importance Resampling* (SIR) is a commonly used technique to transition from a simple distribution to a more complex one. It involves obtaining samples from a target distribution by resampling from a set of samples with weights. These samples are drawn from a proposal distribution, and the weights are adjusted based on the ratio of the target distribution to the proposal distribution. Thus, we could utilize *iterative* SIR (i-SIR) to design efficient global proposal distributions. The likelihood-based i-SIR was originally proposed in Tjelmeland (2004) and further studied in Andrieu et al. (2010, 2018); Samsonov et al. (2022). Here, we introduce a likelihood-free i-SIR as a more efficient global sampler for ABC-MCMC, referred to as ABC-i-SIR. Algorithm 1 illustrates a single stage of ABC-i-SIR. In one stage of ABC-i-SIR, we sample  $\{\boldsymbol{\theta}_{(j)}^*\}_{j=1:N_b}$  from the independent proposal distribution, then generate corresponding synthetic data  $\{\mathbf{x}_{(j)}^*\}_{j=1:N_b}$ . We then combine the newly generated particles with the last state of the chain  $(\boldsymbol{\theta}_{(0)}^*, \mathbf{x}_{(0)}^*) = (\boldsymbol{\theta}_t, \mathbf{x}_t)$  as candidate particles. The new state  $(\boldsymbol{\theta}_{t+1}, \mathbf{x}_{t+1})$  is obtained by sampling from the candidate particles  $\{\boldsymbol{\theta}_{(j)}^*, \mathbf{x}_{(j)}^*\}_{j=0:N_b}$  with importance weights  $w_j \propto \pi(\boldsymbol{\theta}_{(j)}^*)K_\varepsilon(\mathbf{x}_{(j)}^*, \mathbf{y})/q(\boldsymbol{\theta}_{(j)}^*)$ . In Proposition 1 and 2 of Section 2.5, we show that the ABC-i-SIR algorithm can be interpreted as a systematic-scan two-stage Gibbs sampler and demonstrate the uniform geometric ergodicity of the ABC-i-SIR kernel.

---

**Algorithm 1** Single stage of ABC-i-SIR algorithm

---

**Procedure** ABC-i-SIR( $(\boldsymbol{\theta}_t, \mathbf{x}_t)$ ,  $q$ ,  $\pi$ ,  $P_{\boldsymbol{\theta}}$ ,  $K_{\varepsilon}$ )

**Input:** Previous state  $(\boldsymbol{\theta}_t, \mathbf{x}_t)$ , proposal  $q(\cdot)$ , simulator  $P_{\boldsymbol{\theta}}$ , kernel function  $K_{\varepsilon}$ , prior  $\pi(\boldsymbol{\theta})$ .

**Output:** New state  $(\boldsymbol{\theta}_{t+1}, \mathbf{x}_{t+1})$ .

- 1: Set  $(\boldsymbol{\theta}_{(0)}^*, x_{(0)}^*) = (\boldsymbol{\theta}_t, \mathbf{x}_t)$ , draw  $\boldsymbol{\theta}_{(1:N_b)}^*$  from  $q(\cdot)$ .
  - 2: Generate synthetic data  $\mathbf{x}_{(i)}^*$  from  $P_{\boldsymbol{\theta}_{(i)}^*}$  for  $i = 1, \dots, N_b$ .
  - 3: Compute weight  $w_i \propto \pi(\boldsymbol{\theta}_{(i)}^*)K_{\varepsilon}(\mathbf{x}_{(i)}^*, \mathbf{y})/q(\boldsymbol{\theta}_{(i)}^*)$ , for  $i = 0, \dots, N_b$ .
  - 4: Sample  $(\boldsymbol{\theta}_{t+1}, \mathbf{x}_{t+1})$  from  $\left\{(\boldsymbol{\theta}_{(i)}^*, \mathbf{x}_{(i)}^*)\right\}_{i=0:N_b}$  with weight  $\{w_i\}_{i=0:N_b}$ .
- 

## 2.4 Optimization of hyper-parameters

In order to ensure the convergence rate of GL-ABC-MCMC, we need to optimize the hyperparameters (*i.e.* the global frequency  $\gamma$ , the batch size  $N_b$ ). The expected squared jump distance (ESJD) (Pasarica and Gelman, 2010; Atchadé et al., 2011; Roberts and Rosenthal, 2014; Yang et al., 2020) is utilized to adjust the proposal distribution in the MCMC algorithm to improve the algorithm’s mixing and exploration. The ESJD in one dimension is defined as

$$\text{ESJD} = E[|\boldsymbol{\theta}_{t+1} - \boldsymbol{\theta}_t|] = 2(1 - \rho_1) \text{Var}_{\pi_{\varepsilon}}(\boldsymbol{\theta}),$$

where  $\rho_1$  is the first-order autocorrelation of the Markov chain. Maximizing the ESJD is equivalent to minimizing the first-order auto-correlation and thus maximizing the efficiency if the higher-order autocorrelations are monotonically increasing with respect to the first-order auto-correlation (Pasarica and Gelman, 2010). Roberts and Rosenthal (2014) demonstrated that maximizing the ESJD is equivalent to minimizing the asymptotic variance of diffusion limits of MCMC methods in certain scenarios. Yang et al. (2020) considered maximizing ESJD to optimal scaling of random-walk Metropolis algorithms on general target distributions, and showed that the asymptotically optimal acceptance rate 0.234 can be obtained under general realistic sufficient conditions on the target distribution.

For high-dimensional problems, Pasarica and Gelman (2010) defined ESJD as

$$\text{ESJD} = E[\|\boldsymbol{\theta}_{t+1} - \boldsymbol{\theta}_t\|_{\Sigma^{-1}}^2] = 2 \text{tr} \left( I - \Sigma^{-1} E [(\boldsymbol{\theta}_{t+1} - \bar{\boldsymbol{\theta}})(\boldsymbol{\theta}_t - \bar{\boldsymbol{\theta}})^{\top}] \right), \quad (2.3)$$

where  $\bar{\boldsymbol{\theta}}$  and  $\Sigma$  are the mean and covariance matrix of  $\boldsymbol{\theta}$  from the stationary distribution. Maximizing (2.3) is equivalent to minimizing the first-order autocorrelation of the Markov chain. However,

the covariance matrix  $\Sigma$  is typically unknown until the target distribution is well-estimated. In this paper, we define ESJD based on the  $D$ -criterion as follows:

$$\text{ESJD} = |\mathbb{E} [(\boldsymbol{\theta}_{t+1} - \boldsymbol{\theta}_t)(\boldsymbol{\theta}_{t+1} - \boldsymbol{\theta}_t)^\top]|^{\frac{1}{p}} = (|2\Sigma| |I - \Sigma^{-1}E [(\boldsymbol{\theta}_{t+1} - \bar{\boldsymbol{\theta}})(\boldsymbol{\theta}_t - \bar{\boldsymbol{\theta}})^\top]|)^{\frac{1}{p}}, \quad (2.4)$$

where  $p$  is the dimension of  $\boldsymbol{\theta}$ . This accounts for different scales of the parameter dimensions without requiring the estimation of  $\Sigma$ . In extreme cases, Equation (2.4) takes the maximum value  $|2\Sigma|^{1/p}$  when  $\boldsymbol{\theta}_{t+1}$  and  $\boldsymbol{\theta}_t$  are independent, and takes the minimum value 0 when  $\boldsymbol{\theta}_{t+1}$  and  $\boldsymbol{\theta}_t$  are equal. When  $\Sigma$  is a diagonal matrix, Equation (2.4) measures the geometric mean of one-dimensional ESJD from different dimensions. Furthermore, considering the cost associated with different proposal mechanisms, we define a unit cost version of ESJD (cESJD) that accounts for computational cost as follows:

$$\text{cESJD} = \frac{\text{ESJD}}{\mathcal{C}}, \quad (2.5)$$

where  $\mathcal{C}$  denotes the average cost per MCMC iteration (*e.g.* computing time). This ensures a balanced selection of hyper-parameters (*i.e.*  $\gamma$  and  $N_b$ ) that not only maximizes the exploration of the parameter space but also accounts for the efficiency of the MCMC algorithm in terms of computational resources.

To enhance the performance of the GL-ABC-MCMC algorithm, we propose using a sequential optimization algorithm to select an optimal combination of hyper-parameters. This process involves selecting a set of candidate points in the hyper-parameter space based on specific rules, such as informative priors or non-informative uniform density. For each hyper-parameter combination, a short run of the GL-ABC-MCMC algorithm is performed, and the ESJD value is calculated. The best hyper-parameter combination, which yields the highest ESJD, is then used as the center of the parameter space, and the parameter space is narrowed down accordingly. This process is repeated until convergence is achieved or a predetermined requirement is met.

When there is a lack of prior information about hyper-parameters, utilizing uniform design (UD) (Fang et al., 2018) to explore the hyper-parameter space is robust and efficient. UD is constructed based on the number-theoretic method or quasi-Monte Carlo method and possesses good space-filling properties. Yang and Zhang (2021) proposed a method for hyper-parameter optimization via sequential uniform designs. By virtue of its space-filling property, uniform design ensures adequate exploration of the entire parameter space. Compared to random sampling, uniform design can achieve similar exploration effects with fewer sample points, thereby saving



experimental resources and costs. The detailed algorithm is shown in the Supplement S.1.1, Algorithm S.1.

## 2.5 Properties

In this section, we demonstrate that the MCMC kernels of both ABC-i-SIR and GL-ABC-MCMC are  $V$ -uniformly geometrically ergodic under certain mild conditions.

**Notations:** Denote  $\mathbb{N}^* = \mathbb{N} \setminus \{0\}$ . For a measurable function  $f : \mathbb{X} \mapsto \mathbb{R}$ , define  $|f|_\infty = \sup_{x \in \mathbb{X}} |f(x)|$  and  $\pi(f) := \int_{\mathbb{X}} f(x) \pi(dx)$ . For a function  $V : \mathbb{X} \mapsto [1, \infty)$ , we introduce the  $V$ -norm of two probability measures  $\xi$  and  $\xi'$  on  $(\mathbb{X}, \mathcal{X})$ , denoted as  $\|\xi - \xi'\|_V := \sup_{|f(x)| \leq V(x)} |\xi(f) - \xi'(f)|$ . If  $V \equiv 1$ ,  $\|\cdot\|_1$  equals the total variation distance (denoted  $\|\cdot\|_{TV}$ ). For simplicity, we denote the parameter-data pair  $(\boldsymbol{\theta}, \mathbf{x})$  as  $\mathbf{z}$ ,  $\mathbf{z} \in \mathbb{Z} = \Theta \times \mathbb{Y}$ , and the ABC posterior distribution  $\pi_\varepsilon(\boldsymbol{\theta}, \mathbf{x} \mid \mathbf{y})$  as  $\pi_\varepsilon(\mathbf{z})$ , which is defined on the measurable space  $(\mathbb{Z}, \mathcal{Z})$ .

**Definition 1** *A Markov kernel  $Q$  with invariant probability measure  $\pi$  is  $V$ -geometrically ergodic if there exist constants  $\rho \in (0, 1)$  and  $M < \infty$  such that, for all  $x \in \mathbb{X}$  and  $k \in \mathbb{N}$ ,  $\|Q^k(x, \cdot) - \pi\|_V \leq M\{V(x) + \pi(V)\}\rho^k$ .*

In the ABC-i-SIR algorithm, the importance proposal distribution is  $\lambda(\mathbf{z}) \triangleq q(\boldsymbol{\theta})p(\mathbf{x} \mid \boldsymbol{\theta})$ . The Markov chain generated by ABC-i-SIR admits the following Markov kernel:

$$P_{N_b}(\mathbf{z}, A) = \int \delta_{\mathbf{z}}(d\mathbf{z}_{(0)}) \sum_{i=0}^{N_b} \frac{w(\mathbf{z}_{(i)})}{\sum_{j=0}^{N_b} w(\mathbf{z}_{(j)})} 1_A(\mathbf{z}_{(i)}) \prod_{j=0}^{N_b} \lambda(d\mathbf{z}_{(j)}),$$

where  $w(\mathbf{z}) = \pi(\boldsymbol{\theta})p(\mathbf{x} \mid \boldsymbol{\theta})K_\varepsilon(\mathbf{x}, \mathbf{y})/\lambda(\mathbf{z})$  is the unnormalized importance weight function. We denote the function as  $w(\mathbf{z}) = \pi_\varepsilon(\mathbf{z}) \cdot \lambda(w)/\lambda(\mathbf{z})$ , where  $\lambda(w)$  is the normalizing constant of the distribution  $\pi_\varepsilon(\mathbf{z})$ . Next, we present two propositions for the ABC-i-SIR algorithm.

**Proposition 1** *The ABC-i-SIR algorithm can be interpreted as a systematic-scan two-stage Gibbs sampler, that is  $\left\{(\boldsymbol{\theta}_{(i)}^*, \mathbf{x}_{(i)}^*)\right\}_{i=0:N_b} \mid (\boldsymbol{\theta}_t, \mathbf{x}_t) \rightarrow (\boldsymbol{\theta}_{t+1}, \mathbf{x}_{t+1}) \mid \left\{(\boldsymbol{\theta}_{(i)}^*, \mathbf{x}_{(i)}^*)\right\}_{i=0:N_b}$ , and the marginal distribution of  $\left((\boldsymbol{\theta}, \mathbf{x}), \left\{(\boldsymbol{\theta}_{(i)}^*, \mathbf{x}_{(i)}^*)\right\}_{i=0:N_b}\right)$  with respect to  $(\boldsymbol{\theta}, \mathbf{x})$  is  $\pi_\varepsilon(\boldsymbol{\theta}, \mathbf{x} \mid \mathbf{y})$ .*

**Proposition 2** *If  $|w|_\infty < \infty$ , for any initial distribution  $\xi$  on  $(\mathbb{Z}, \mathcal{Z})$  and  $k \in \mathbb{N}$ ,  $\|\xi P_{N_b}^k - \pi_\varepsilon\|_{TV} \leq \rho_{N_b}^k$  with  $\rho_{N_b} = 1 - e_{N_b}$ ,  $e_{N_b} = N_b/(2L + N_b - 1)$ , and  $L = |w|_\infty/\lambda(w)$ .*

Proposition 1 shows that the ABC-i-SIR algorithm operates as a systematic-scan two-stage Gibbs sampler, with the marginal distribution of the target being  $\pi_\varepsilon(\boldsymbol{\theta}, \mathbf{x} \mid \mathbf{y})$ . Proposition 2 establishes that the MCMC kernel of ABC-i-SIR  $P_{N_b}$  is  $V$ -geometrically ergodic. Here, the assumption  $|w|_\infty < \infty$  implies that the importance proposal must cover the target distribution, that is,  $q(\boldsymbol{\theta}) > 0$  for all  $\boldsymbol{\theta} \in \{\boldsymbol{\theta} : \pi_\varepsilon(\boldsymbol{\theta} \mid \mathbf{y})\}$ , which is a standard assumption for importance sampling. In practice, it suffices to set the importance proposal to cover the prior region. The proofs of Propositions 1 and 2 are shown in the Supplement S.2.1 and S.2.2.

**Assumption 1** (i) *The local Markov kernel  $Q$  has  $\pi_\varepsilon$  as its unique invariant distribution;*

(ii) *There exists a function  $V : \mathbf{z} \rightarrow [1, \infty)$ , such that for all  $r \geq r_Q > 1$  there exist  $\zeta_{Q,r} \in [0, 1)$ ,  $b_{Q,r} < \infty$ , such that  $QV(\mathbf{z}) \leq \zeta_{Q,r}V(\mathbf{z}) + b_{Q,r}\mathbb{I}_{V_r}$ , where  $V_r = \{\mathbf{z} : V(\mathbf{z}) \leq r\}$ .*

**Assumption 2** *For all  $r \geq r_Q$ ,  $w_{\infty,r} := \sup_{\mathbf{z} \in V_r} \{w(\mathbf{z})/\lambda(w)\} < \infty$  and  $\text{Var}_\lambda(w)/\{\lambda(w)\}^2 \leq \infty$ .*

**Theorem 1** *Under the Assumptions 1 and 2, then for all  $z \in \mathbb{Z}$ ,  $k \in \mathbb{N}$ , and  $N_b \geq 2$*

$$\|K_{N_b}^k(\mathbf{z}, \cdot) - \pi_\varepsilon(\cdot)\|_V \leq c_{K_{N_b}} \{\pi_\varepsilon(V) + V(\mathbf{z})\} \rho_{K_{N_b}}^k, \quad (2.6)$$

with

$$\begin{aligned} \log \rho_{K_{N_b}} &= \frac{\log(1 - e_{K_{N_b}}) \log \bar{\zeta}_{K_{N_b}}}{\log(1 - e_{K_{N_b}}) + \log \bar{\zeta}_{K_{N_b}} - \log \bar{b}_{K_{N_b}}}, \\ c_{K_{N_b}} &= 1 + \bar{b}_{K_{N_b}} / \left[ (1 - e_{K_{N_b}})(1 - \bar{\zeta}_{K_{N_b}}) \right], \\ \bar{\zeta}_{K_{N_b}} &= \zeta_{K_{N_b}} + 2b_{K_{N_b}} / (1 + r_{K_{N_b}}), \quad \bar{b}_{K_{N_b}} = \zeta_{K_{N_b}} r_{K_{N_b}} + b_{K_{N_b}}. \end{aligned}$$

where  $K_{N_b} = \gamma P_{N_b} + (1 - \gamma)Q$  with  $\gamma \in (0, 1]$ .

Theorem 1 establishes that the kernel of GL-ABC-MCMC is  $V$ -uniformly geometrically ergodic under Assumptions 1 and 2. Specifically, Assumption 1(ii) requires that the Markov kernel  $Q$  satisfies a Foster-Lyapunov drift condition for the function  $V$ , which is commonly met by traditional MCMC kernels like the Metropolis-Hastings kernel. Assumption 2 stipulates that the (normalized) importance weights are upper bounded on the sets  $V_r$ . This is considered as a mild condition: if  $\mathbb{Z} = \mathbb{R}^d$  and  $V$  is norm-like, then the level sets  $V_r$  are compact, and  $w(\cdot)$  is bounded on  $V_r$  as long as the importance proposal covers the prior region. The condition  $\text{Var}_\lambda(w)/\{\lambda(w)\}^2 \leq \infty$  implies that the variance of the importance weights is bounded, which corresponds to the  $\chi^2$ -distance

between the proposal and target distributions, playing a crucial role in the performance of SIR methods. Notably, Assumptions 1 and 2 do not require the identification of small sets for the rejuvenation kernel  $Q$ , which is a necessary condition for the local kernel  $Q$  to satisfy  $V$ -geometric ergodicity. Finally, Theorem 1 implies that the mixing rate  $\rho_{K_{N_b}}^k$  of the GL-ABC-MCMC kernel  $K_{N_b}$  exceeds that of the local kernel  $Q$  in some sense.

### 3 Two adaptive schemes

In this section, we propose two adaptive schemes for ABC-i-SIR and local proposals to improve the inference of complex models.

#### 3.1 An adaptive global proposal with normalizing flows

In Section 2.3, we employ the likelihood-free SIR technique iteratively to construct an efficient global kernel for ABC-MCMC. The proposal distribution plays a crucial role in importance sampling, influencing the efficiency of the sampling process. Essentially, the proposal determines where samples are drawn from, and its similarity to the target distribution significantly impacts the quality of estimates. An effective proposal reduces variability and yields more reliable results. The calculation of weights depends on how well the proposal aligns with the target, and optimal performance is achieved when the proposal closely approximates the target distribution. In this section, we enhance the importance proposal distribution of ABC-i-SIR to closely match the target distribution by training a normalizing flow throughout the sampling process.

Let  $u \in \mathbb{R}^d$  be a random variable with a known and tractable probability density function  $p_B$ . Suppose  $T$  is an invertible and differentiable function; then the density of  $\nu = T(u)$  can be evaluated by

$$p_T(\nu) = p_B(f(\nu))|\det \nabla f(\nu)| = p_B(f(\nu))|\det \nabla T(f(\nu))|^{-1}, \quad (3.7)$$

where  $f$  is the inverse function of  $T$  (*i.e.*  $u = f(T(u))$ ),  $\nabla f(\nu) = \partial f(\nu)/\partial \nu$  and  $\nabla T(u) = \partial T(u)/\partial u$ . Intuitively, if the transformation  $T$  can be arbitrarily complex, we can generate any distribution  $p_T$  from any base distribution  $p_B$ . A normalizing flow is a transformation of a simple distribution into a complex one by the composition of a sequence of invertible and differentiable functions. In order to generate our target distribution, we often parameterize a flow  $T$  with

parameter  $\beta$ , and obtain an optimal invertible map  $T^*$  by minimizing the KL divergence between the ABC posterior  $\pi_\varepsilon(\boldsymbol{\theta} \mid \mathbf{y})$ , that is,

$$D_{\text{KL}}^{\text{F}}(\pi_\varepsilon \parallel p_T) = C - \int_{\Theta} \pi_\varepsilon(\boldsymbol{\theta} \mid \mathbf{y}) \log p_T(\boldsymbol{\theta}) d\boldsymbol{\theta}, \quad (3.8)$$

where  $C = \int_{\Theta} \log(\pi_\varepsilon(\boldsymbol{\theta} \mid \mathbf{y})) \pi_\varepsilon(\boldsymbol{\theta} \mid \mathbf{y}) d\boldsymbol{\theta}$  is a constant irrelevant to optimization of  $T$ . The integral in Equation (3.8) can be approximated by Monte Carlo methods. In practice, we employ gradient descent to optimize the KL divergence, aiming to iteratively update the parameters of  $T$ . Here, we employ the forward KL  $D_{\text{KL}}^{\text{F}}(\pi_\varepsilon \parallel p_T)$  instead of the backward KL divergence  $D_{\text{KL}}^{\text{F}}(p_T \parallel \pi_\varepsilon)$  because the former seeks to cover or average the probability mass, whereas the latter seeks to match the modes, that is, forcing distributions to align at specific points of high probability. Relying solely on gradients from the backward KL divergence is susceptible to mode-collapse if samples from the base distribution cannot adequately cover the space of the target distribution (Gabri  et al., 2022; Parno and Marzouk, 2018).

To estimate of gradient of  $D_{\text{KL}}^{\text{F}}(\pi_\varepsilon \parallel p_T)$ , evaluating  $p_T(\boldsymbol{\theta})$  is straightforward. However, obtaining samples from  $\pi_\varepsilon$  poses a challenge. Gabri  et al. (2022) suggest running  $M$  parallel Markov chains, using their samples at each iteration as approximate samples from  $\pi_\varepsilon$ . This method, however, demands more computational resources than running a single chain. Here, we propose a novel approach that fully recycles all  $N$  candidates sampled at each iteration of ABC-i-SIR. We treat the weighted particles  $\{\theta_{t,i}^*, w_{t,i}\}$  as the samples from  $\pi_\varepsilon$ . These particles  $\{\theta_{t,i}^*, w_{t,i}\}$  are then employed to approximate the integral in  $D_{\text{KL}}^{\text{F}}(\pi_\varepsilon \parallel p_T)$  (*i.e.*, the loss function of  $T$ ),

$$L(T; \{\theta_{t,i}^*, w_{t,i}\}) = - \sum_{i=1}^N w_i \log(p_T(\theta_{t,i}^*)).$$

The constant  $C$  in Equation (3.8) is omitted here since it does not affect the optimization of  $T$ . Algorithm 2 outlines a single stage of ABC-i-SIR algorithm enhanced with NF.

## 3.2 A gradient based local proposal

In practice, it is common to employ a  $p$ -dimensional normal distribution as a proposal for local MCMC steps (*e.g.*,  $q(\boldsymbol{\theta}^* \mid \boldsymbol{\theta}) = \mathcal{N}(\boldsymbol{\theta}^*; \boldsymbol{\theta}, \sigma^2 \mathbf{I}_p)$ ). The scale parameter of the normal distribution significantly influences the efficiency and performance of the algorithm, especially in high-dimensional parameter spaces. Designing an appropriate scale poses a challenge. It’s necessary to

---

**Algorithm 2** Single stage of ABC-i-SIR augmented with NF

---

**Procedure** ABC-i-SIR-NF( $(\boldsymbol{\theta}_t, \mathbf{x}_t)$ ,  $q$ ,  $P_{\boldsymbol{\theta}}$ ,  $K_{\varepsilon}$ ). **Input:** Previous state  $(\boldsymbol{\theta}_t, \mathbf{x}_t)$ , normalizing flow  $T$ , simulator  $P_{\boldsymbol{\theta}}$ , kernel  $K_{\varepsilon}$ , prior  $\pi(\boldsymbol{\theta})$ , step size of gradient descent  $r$ , number of steps to collect data  $S$ .

**Output:** New state  $(\boldsymbol{\theta}_{t+1}, \mathbf{x}_{t+1})$ , map  $T$ .

- 1:  $\boldsymbol{\theta}_{(0)}^* = \boldsymbol{\theta}_t$ , draw  $\boldsymbol{\theta}_{(1:N_b)}^*$  from  $p_T(\cdot)$ .
  - 2: Generate simulate data  $\mathbf{x}_{(i)}^*$  from  $P_{\boldsymbol{\theta}_{(i)}^*}$  for  $i = 0, \dots, N_b$ .
  - 3: Compute weight  $w_i = w(\boldsymbol{\theta}_{(i)}^*) / \sum_{i=1}^{N_b} w(\boldsymbol{\theta}_{(i)}^*)$ , for  $i = 0, \dots, N_b$ , where  $w(\boldsymbol{\theta}_{(i)}^*) = \pi(\boldsymbol{\theta}_{(i)}^*) K_{\varepsilon}(\mathbf{x}_{(i)}^*, \mathbf{y}) / q(\boldsymbol{\theta}_{(i)}^*)$ . Collect  $\{(\boldsymbol{\theta}_{(i)}^*, w(\boldsymbol{\theta}_{(i)}^*))\}_{i=1:N_b}$  into the train data set  $\mathcal{D}$ .
  - 4: Sample  $\boldsymbol{\theta}_{t+1}$  from  $\{\boldsymbol{\theta}_{(i)}^*\}_{i=0:N_b}$  with weight  $\{w_i\}_{i=0:N_b}$ .
  - 5: **if**  $t \bmod S = 0$  **then**
    - 6: Normalize the weight in  $\mathcal{D}$ ,  $W_i = w(\boldsymbol{\theta}_{(i)}^*) / \sum_{i=1}^{S \cdot N_b} w(\boldsymbol{\theta}_{(i)}^*)$ , for  $i = 1, \dots, S \cdot N_b$ .
    - 7: Compute  $L(T) = - \sum_{i=1}^{S \cdot N_b} W_i \log(p_T(\boldsymbol{\theta}_{(i)}^*))$ , update the parameter  $\beta$  of  $T$ ,  $\beta \leftarrow \beta - r \nabla_{\beta} L(T)$ .
  - 8: Initialize  $\mathcal{D}$  to an empty set.
  - 9: **end if**
- 

design a general proposal mechanism which provides large proposal transitions with a high probability of acceptance. *Metropolis adjusted Langevin algorithm* (MALA) (Grenander and Miller, 1994; Roberts and Tweedie, 1996; Roberts and Rosenthal, 1998; Girolami and Calderhead, 2011) combines Langevin dynamics with a Metropolis-Hastings correction to create an adaptive and efficient MCMC algorithm.

The Langevin diffusion process is defined by the stochastic differential equation (SDE):

$$d\boldsymbol{\theta}(t) = \nabla_{\boldsymbol{\theta}} \mathcal{L}\{\boldsymbol{\theta}(t)\} dt / 2 + d\mathbf{W}(t), \quad (3.9)$$

where  $\mathcal{L}(\boldsymbol{\theta})$  denotes the logarithm of target distribution, and  $\mathbf{W}$  denotes a  $p$ -dimensional Brownian motion. The diffusion is irreducible, strong Feller and aperiodic, with stationary distribution  $\pi_T(\cdot) \propto \exp(\mathcal{L}(\cdot))$ . This process can be regarded as a continuous-time sampling method. Unfortunately, its implementation is infeasible in practice. The common method is to use discretized approximations via Euler-Maruyama discretization:

$$\boldsymbol{\theta}^* = \boldsymbol{\theta} + \eta^2 \nabla_{\boldsymbol{\theta}} \mathcal{L}(\boldsymbol{\theta}) / 2 + \eta z, \quad (3.10)$$

where  $\eta$  is the step-size and  $z \sim \mathcal{N}(0, \mathbf{I}_p)$ . However, when discretizing the diffusion, some bias is introduced, and convergence to the invariant distribution  $\pi_T$  is no longer guaranteed. MALA employs a Metropolis-Hastings rejection-acceptance step after every iteration to ensure the convergence property. The discrete form of Langevin diffusion serves as an instrumental proposal distribution. In particular,  $q(\boldsymbol{\theta}^* | \boldsymbol{\theta}) = \mathcal{N}\{\boldsymbol{\theta} | \boldsymbol{\theta} + \eta^2 \nabla_{\boldsymbol{\theta}} \mathcal{L}(\boldsymbol{\theta})/2, \eta^2 \mathbf{I}_p\}$  and the corresponding acceptance probability is  $\alpha(\boldsymbol{\theta}, \boldsymbol{\theta}^*) = \min\left\{1, \frac{\exp(\mathcal{L}(\boldsymbol{\theta}^*))q(\boldsymbol{\theta}|\boldsymbol{\theta}^*)}{\exp(\mathcal{L}(\boldsymbol{\theta}))q(\boldsymbol{\theta}^*|\boldsymbol{\theta})}\right\}$ .

Our target distribution is defined as  $\pi_{\varepsilon}(\boldsymbol{\theta} | \mathbf{y}) \propto \pi(\boldsymbol{\theta})p_{\varepsilon}(\mathbf{y} | \boldsymbol{\theta})$ , where  $p_{\varepsilon}(\mathbf{y} | \boldsymbol{\theta}) = \int p(\mathbf{x} | \boldsymbol{\theta})K_{\varepsilon}(\mathbf{x}, \mathbf{y})d\mathbf{x}$  represents the approximate likelihood. This leads to the formulation  $\mathcal{L}(\boldsymbol{\theta}) = \log(\pi(\boldsymbol{\theta})) + \log(p_{\varepsilon}(\mathbf{y} | \boldsymbol{\theta}))$ . A critical component of ABC-MALA is computing the gradient of log-likelihood. Meeds et al. (2015) applied HMC to ABC, proposing *common random numbers* (CRN) for gradient computation. The CRN approach involves representing  $\mathbf{x}$  as a deterministic function of variables  $\boldsymbol{\theta}$  and  $\omega$ , defining the random variable  $\mathbf{x}$  from  $p(\mathbf{x} | \boldsymbol{\theta})$  as a function  $f(\boldsymbol{\theta}, \omega)$ , where  $\omega$  is a random seed. Then, the estimated likelihood based on  $\varepsilon$ -kernel is

$$p_{\varepsilon}(\mathbf{y} | \boldsymbol{\theta}) = \sum_{s=1}^S K_{\varepsilon}(f(\boldsymbol{\theta}, \omega_s), \mathbf{y}), \quad (3.11)$$

where  $\omega_s$  ( $s = 1, \dots, S$ ) are  $S$  random seeds. Meeds et al. (2015) suggest approximating the conditional distribution  $p_{\varepsilon}(\mathbf{y} | \boldsymbol{\theta})$  by  $K_{\varepsilon}(f(\boldsymbol{\theta}, \omega_m), \mathbf{y})$  under the assumption of a very small threshold,  $\varepsilon$ . Here,  $\omega_m$  is the seed that ensures  $K_{\varepsilon}(f(\boldsymbol{\theta}, \omega_m), \mathbf{y})$  is the largest among  $\{K_{\varepsilon}(f(\boldsymbol{\theta}, \omega_i), \mathbf{y})\}_{i=1:S}$ . The gradient of log-likelihood is then estimated by

$$\nabla_{\boldsymbol{\theta}} \log(p_{\varepsilon}(\mathbf{y} | \boldsymbol{\theta})) = \frac{\log(K_{\varepsilon}(f(\boldsymbol{\theta} + d_{\boldsymbol{\theta}}, \omega_m^+), \mathbf{y})) - \log(K_{\varepsilon}(f(\boldsymbol{\theta} - d_{\boldsymbol{\theta}}, \omega_m^-), \mathbf{y}))}{2d_{\boldsymbol{\theta}}}, \quad (3.12)$$

where  $\omega_m^+ = \arg \max_{\omega_i \in \{\omega_{1:S}\}} K_{\varepsilon}(f(\boldsymbol{\theta} + d_{\boldsymbol{\theta}}, \omega_i), \mathbf{y})$  and  $\omega_m^- = \arg \max_{\omega_i \in \{\omega_{1:S}\}} K_{\varepsilon}(f(\boldsymbol{\theta} - d_{\boldsymbol{\theta}}, \omega_i), \mathbf{y})$ . This method is denoted as  $\text{CRN}_{max}$ . In practice, achieving efficient ABC methods with a very small  $\varepsilon$  is challenging. Here, we estimate the partial derivative with respect to  $\boldsymbol{\theta}$  without assuming a small threshold as follows:

$$\nabla_{\boldsymbol{\theta}} \log(p_{\varepsilon}(\mathbf{y} | \boldsymbol{\theta})) = \frac{\log\left(\sum_{s=1}^S K_{\varepsilon}(f(\boldsymbol{\theta} + d_{\boldsymbol{\theta}}, \omega_s), \mathbf{y})\right) - \log\left(\sum_{s=1}^S K_{\varepsilon}(f(\boldsymbol{\theta} - d_{\boldsymbol{\theta}}, \omega_s), \mathbf{y})\right)}{2d_{\boldsymbol{\theta}}}, \quad (3.13)$$

where  $d_{\boldsymbol{\theta}}$  is a small perturbation. The detailed finite difference stochastic approximation with CRN ( $\text{CRN}_{mean}$ ) is shown in the Supplement S.1.2.

However, in the tail region of the posterior distribution, the logarithmic function can amplify errors associated with Monte Carlo integration, leading to significantly inaccurate gradient estimates. To address this, we employ a Gaussian distribution to model the likelihood based on simulated data, achieving a more stable and accurate estimator when simulations are scarce for estimating the integral. By utilizing the Gaussian kernel as the kernel density function, we derive the gradient estimate as follows:

$$\nabla_{\boldsymbol{\theta}} \log(p_{\varepsilon}(\mathbf{y} \mid \boldsymbol{\theta})) = \frac{1}{2d_{\boldsymbol{\theta}}} \left( -\frac{1}{2} \log \left( \frac{\hat{\sigma}_{\boldsymbol{\theta}^+}^2 + \varepsilon^2}{\hat{\sigma}_{\boldsymbol{\theta}^-}^2 + \varepsilon^2} \right) - \frac{(\mathbf{y} - \hat{\boldsymbol{\mu}}_{\boldsymbol{\theta}^+})^2}{2(\hat{\sigma}_{\boldsymbol{\theta}^+}^2 + \varepsilon^2)} + \frac{(\mathbf{y} - \hat{\boldsymbol{\mu}}_{\boldsymbol{\theta}^-})^2}{2(\hat{\sigma}_{\boldsymbol{\theta}^-}^2 + \varepsilon^2)} \right), \quad (3.14)$$

where the mean  $\hat{\boldsymbol{\mu}}_{\boldsymbol{\theta}^+}$  and variance  $\hat{\sigma}_{\boldsymbol{\theta}^+}^2$  are estimated from samples drawn from the distribution  $p(\cdot \mid \boldsymbol{\theta} + d\boldsymbol{\theta})$ , while mean  $\hat{\boldsymbol{\mu}}_{\boldsymbol{\theta}^-}$  and variance  $\hat{\sigma}_{\boldsymbol{\theta}^-}^2$  are derived similarly. Samples from  $p(\cdot \mid \boldsymbol{\theta} + d\boldsymbol{\theta})$  and  $p(\cdot \mid \boldsymbol{\theta} - d\boldsymbol{\theta})$  are generated using a common random seed.

## 4 Toy examples

### 4.1 Comparison of different gradient estimation methods

We use a simple one-dimensional problem to illustrate the effectiveness of the gradient estimation method proposed in this article. We consider a model with the prior density  $\pi(\theta) = \mathcal{N}(\theta; 0, 1)$ , the likelihood function  $p(y \mid \theta) = \mathcal{N}(y; \theta, 0.01)$ , the observation  $y_{obs} = 0$ , and the weighted kernel function  $K_{\varepsilon}(x, y_{obs}) = \mathcal{N}(x; y_{obs}, \varepsilon^2)$ , where  $\mathcal{N}(\theta, \mu, \sigma^2)$  denotes a Gaussian density with mean  $\mu$  and variance  $\sigma^2$ . The closed expression of estimated likelihood and gradient based on  $\varepsilon$ -kernel are  $p_{\varepsilon}(y \mid \theta) = \mathcal{N}(y, \theta, \varepsilon^2 + 0.01)$ , and  $\nabla_{\theta} \log p_{\varepsilon}(y \mid \theta) = (y - \theta)/(\varepsilon^2 + 0.01)$ .

In Supplement S.3.1, we demonstrate that for a fixed random seed  $\omega_s$ , the simulation data  $y$  is deterministic for a given  $\theta$  and varies smoothly with changes of  $\theta$ , despite the inherent noise in the simulator. For numerical methods, we fixed  $d_{\theta} = 0.05$ . Figure 1 provides gradient estimates obtained from various methods. For each parameter value, gradients are estimated using 100 simulated data points, and the process is repeated 1,000 times to calculate both the mean and standard deviation of the gradient estimates.

Compared to the standard method (random sampling) and the  $CRN_{max}$  approach (Meeds et al., 2015), the  $CRN_{mean}$  method significantly reduces the variance of the estimates and provides more accurate estimates in regions with high likelihood values. However, in regions where  $p_{\varepsilon}(y \mid \theta)$

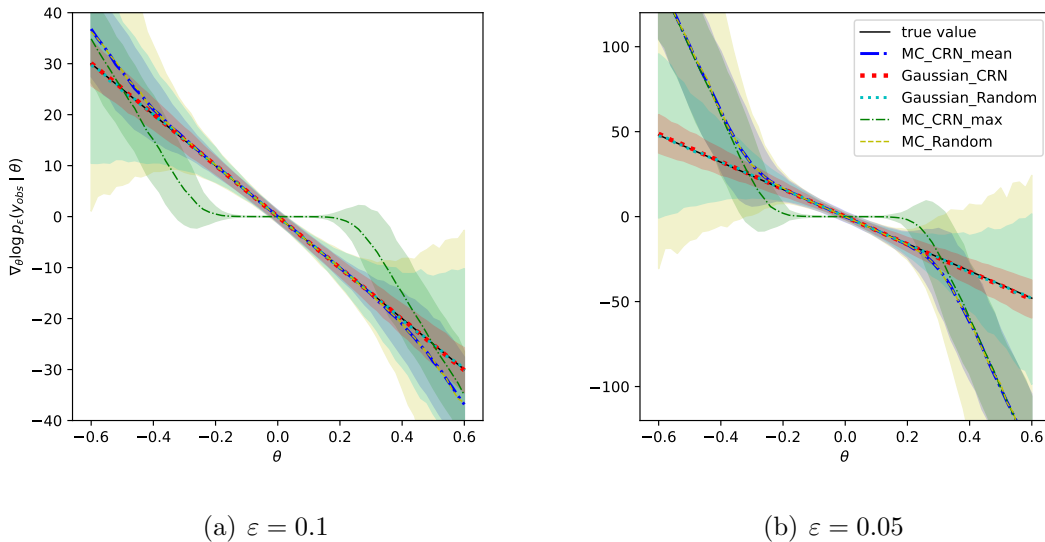


Figure 1: Comparison of gradient estimation methods. The shaded region represents  $2\sigma$  of estimated gradient. The standard method (MC\_Random), the method of Meeds et al. (2015) (MC\_CRN\_max, Eq. (3.12)), the improved method based on Meeds et al. (2015) (MC\_CRN\_mean, Eq. (3.13)), the likelihood fitting using Gaussian distribution based on simulation data with CRNs (Gaussian\_CRN, Eq. (3.14) with CRNs), and the likelihood fitting using Gaussian distribution based on random simulation data (Gaussian\_Random, Eq. (3.14)) are compared.

approaches zero, substantial deviations are observed because the logarithmic function amplifies the errors in the Monte Carlo estimates. By employing the CRNs technique, fitting a Gaussian density can significantly enhance both the accuracy and variance of the estimates.

## 4.2 Three synthetic probability densities

We illustrate the advantages of our approach through three synthetic examples: Mixture Gaussian, Moon and Wave shaped posterior. The visualization of these posterior densities are shown in Figure 2. In this simulation, MCMC with a local proposal involves generating candidate particle  $\theta^*$  from a normal distribution  $N(\theta_{t-1}, \sigma^2)$  at the  $t$ -th iteration. On the other hand, MCMC with a global proposal (MCMCg) generates candidate particle  $\theta^*$  from a proposal distribution  $q(\cdot)$  that is independent with  $\theta_{t-1}$ , at the  $t$ -th iteration. The true ABC posterior is estimated using  $5 \times 10^5$  samples, obtained by running importance sampling with  $10^8$  samples from the prior. We use



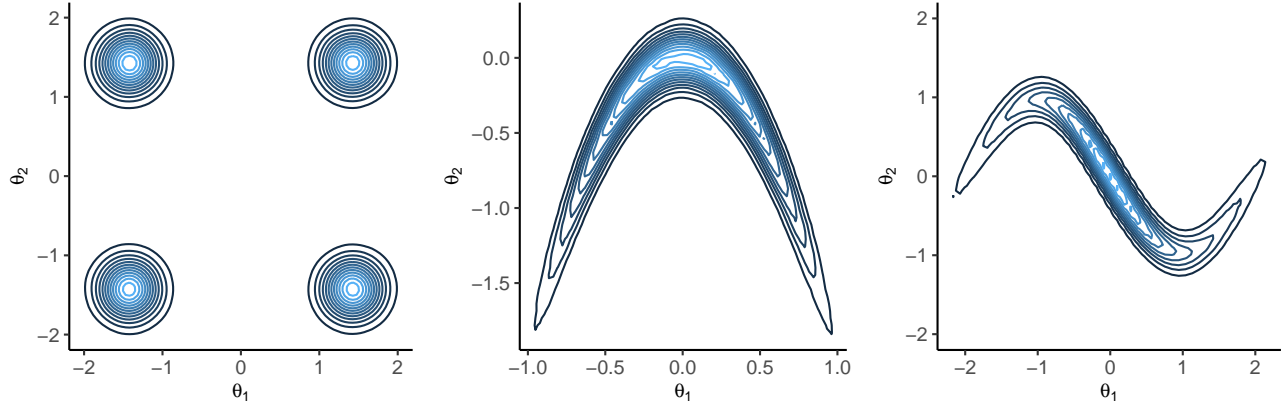


Figure 2: Posterior probability density illustration for three synthetic test functions. Labels of the test functions from left to right: Mixture Gaussian, Moon and Wave.

the `bkde2D` function from the R package *KernelSmooth* (Wand, 1994) to estimate the posterior density based on the posterior samples. The accuracy of different methods is measured by the KL divergence between the estimated posterior and the true posterior, calculated as

$$D_{KL}(\pi_\varepsilon \mid \hat{\pi}_\varepsilon) = \frac{1}{|\Theta_{ref}|} \sum_{\boldsymbol{\theta} \in \Theta_{ref}} \pi_\varepsilon(\boldsymbol{\theta} \mid \mathbf{y}) \log \frac{\pi_\varepsilon(\boldsymbol{\theta} \mid \mathbf{y})}{\hat{\pi}_\varepsilon(\boldsymbol{\theta} \mid \mathbf{y})},$$

where  $\pi_\varepsilon$  is the true ABC posterior density and  $\hat{\pi}$  is the estimated ABC posterior density. In Figure 2,  $\Theta_{ref}$  is generated in a two-dimensional grid of  $501^2$  points on the posterior region, that is  $[-3, 3] \times [-3, 3]$  of Mixture,  $[-2, 2] \times [-5, 1]$  of Moon, and  $[-1, 1] \times [-4, 4]$  of Wave. More details of each simulation model are provided in Supplement S.3.2.

Firstly, we utilize the Mixture example to illustrate how ABC-i-SIR can improve the mixing of ABC-MCMC with local proposals, which often fails to switch effectively between peaks. Figure 3 displays a segment of the trace plots (*i.e.*, iteration 30,001  $\sim$  40,000) for three MCMC methods: ABC-MCMC with a Gaussian proposal (left), ABC-MCMC with prior distribution as the global proposal (middle), and ABC-i-SIR with prior distribution as the importance proposal, with batch size 51 (right). The analysis reveals that ABC-MCMC with local proposals struggles to transition efficiently between peaks, while ABC-MCMC samplers with global proposals can traverse between peaks, their efficiency in exploring the local posterior region is notably low. In contrast, the ABC-i-SIR algorithm demonstrates that its particles are capable of both traversing between peaks and effectively exploring the posterior region.

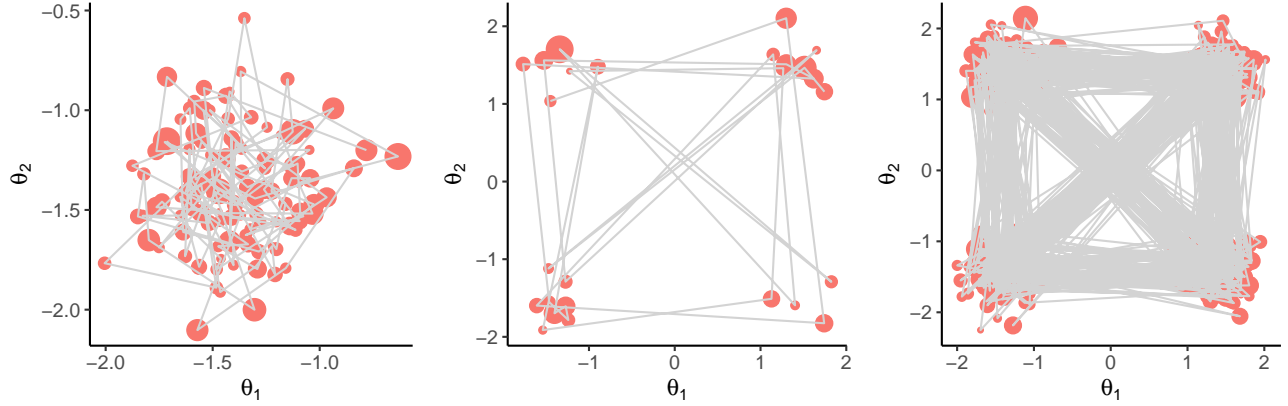


Figure 3: Trace plots of three ABC-MCMC methods for the mixture of Gaussian example: ABC-MCMC with a local proposal (left), ABC-MCMC with the prior distribution as global proposal (middle) and ABC-i-SIR with the prior distribution as the proposal and the batch size is 51 (right). The red dots and their size represent location and number of particles, the grey lines depict the movement trajectories.

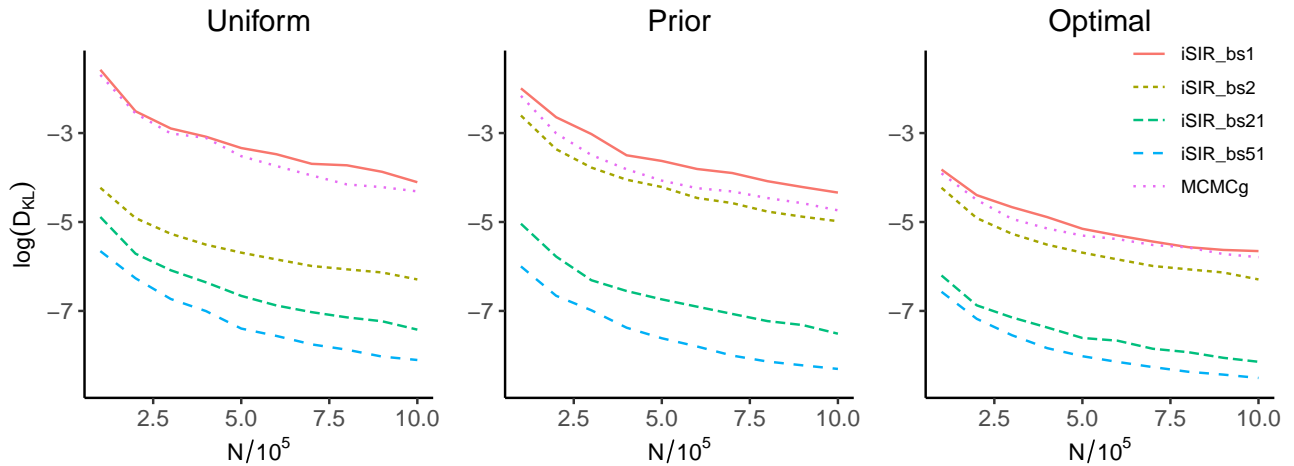


Figure 4: Comparison of ABC-i-SIR and MCMC with different proposals and batch sizes for Mixture Gaussian. “Optimal”: a proposal close to the ABC posterior, “Uniform”: a uniform proposal, “Prior” : the prior distribution as proposal.

Additionally, we employ the Mixture example to investigate the influence of various proposal distributions and batch size on the performance of ABC-i-SIR. We use three different distributions as the global proposal of MCMC and the importance proposal of ABC-i-SIR respec-

tively. There are, Uniform:  $U(-4, 4)^2$ , Prior:  $N(0, I_2)$  and Optimal:  $(N((1.425, 1.425)^\top, 0.28^2 I) + N((-1.425, 1.425)^\top, 0.28^2 I) + N((1.425, -1.425)^\top, 0.28^2 I) + N((-1.425, -1.425)^\top, 0.28^2 I))/4$ .

Figure 4 shows that the accuracy of the ABC-i-SIR algorithm increases with the batch size. The selection of proposal distributions impacts the convergence speed of the ABC-i-SIR algorithm, but this effect diminishes as the batch size increases. This indicates that we can improve the performance of the algorithm by increasing the batch size when it is difficult to construct a good proposal distribution, which could be highly advantageous for parallel simulation models. Notably, ABC-MCMC with global proposals outperforms ABC-i-SIR with batch size 1.

In cases where generating simulation data is constrained, we can collect training data during the algorithm’s iterative process and employ normalizing flows to enhance the proposal distribution. Figure 5 demonstrates that NFs can significantly improve the algorithm’s convergence speed. Here the proposal is the prior distribution, and we update the NF model every time we collect 1000 simulated data points, with a total of 50 updates.

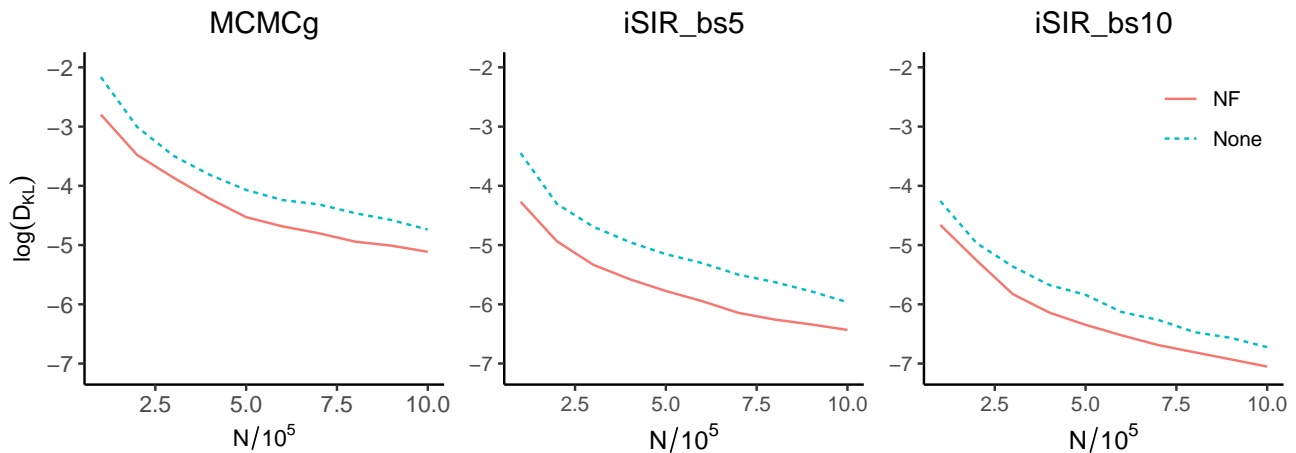


Figure 5: Comparison of different methods on whether to perform NFs training. ‘MCMC<sub>g</sub>’: MCMC with a global proposal. ‘iSIR<sub>bsi</sub>’: iSIR with batch size  $i$ . Dashed line: methods with NF, solid line: methods without NFs.

Tables 1 presents a comparison of several ABC-MCMC methods for the Mixture, Moon, and Wave examples. GL-ABC-MCMCs are the combinations of MALA and ABC-i-SIR, using the prior distribution as the importance proposal. The step size of MALA is chosen using a sequential optimal algorithm based on ESJD. Notably, GL-ABC-MCMC degenerates into MALA when

$\gamma = 0$  and into ABC-i-SIR when  $\gamma = 1.0$ . Each MCMC algorithm was repeated 10 times, with 1,000,000 iterations per run. Table 1 shows the KL divergences between the estimated posterior of different ABC-MCMC methods and the ground truth, along with their standard deviations. In the three examples, the combination of global proposal and local proposal demonstrated superior performance compared to ordinary ABC-MCMC and MALA algorithms, especially in the case of the multi-modal Mixture example. Compared to the standard MCMC algorithm, the MALA algorithm, which utilizes the gradient of the log-likelihood function, achieved a more accurate posterior estimate and a larger effective sample size. This was especially true for models with posterior distributions exhibiting strong correlations, such as Moon and Wave examples (detailed results can be seen in Supplement S.3.2, Table S.1). When using a batch size of 5, the GL-ABC-MCMC algorithm with  $\gamma = 0.4$  in the Mixture example and  $\gamma = 0.8$  in the Moon example performed the best. This suggests that the combination of global and local proposals may be particularly effective when the global exploration ability of the algorithm is relatively weak.

Table 1: The KL divergence between the estimated posterior of different ABC-MCMC methods and the ground truth for Moon and Banana data sets.  $\gamma$  denotes global frequency and ‘bs<sub>*i*</sub>’ denotes batch size *i*.

Method	Mixture ( $10^{-3}(10^{-4})$ )		Moon ( $10^{-3}(10^{-4})$ )		Wave ( $10^{-5}(10^{-6})$ )		
	$\gamma$	bs <sub>5</sub>	bs <sub>10</sub>	bs <sub>5</sub>	bs <sub>10</sub>	bs <sub>5</sub>	bs <sub>10</sub>
GL-ABC-MCMC	0.2	2.4(2.3)	1.9(2.0)	1.9(9.1)	1.3(5.1)	12.1(26.3)	9.7(14.5)
	0.4	<b>2.1</b> (2.2)	1.6(1.2)	1.4(4.9)	0.7(2.1)	11.3(24.7)	6.7(6.3)
	0.6	2.2(2.1)	1.4(1.4)	1.2(2.9)	0.7(1.9)	8.4(9.0)	5.2(3.5)
	0.8	2.3(1.8)	1.3(1.0)	<b>0.9</b> (3.1)	0.6(1.9)	7.2(8.0)	4.1(4.1)
	1.0	2.4(1.6)	<b>1.2</b> (0.7)	1.1(2.2)	<b>0.4</b> (0.7)	<b>6.5</b> (5.9)	<b>3.6</b> (3.6)
MCMC	1658.5(1145.9)		13.1(85.4)		63.1(470.7)		
MALA	1650.0(922.0)		5.9 (33.3)		18.3(86.6)		

## 5 Real Examples

### 5.1 Example 1: Roman binary microlensing events

A binary-lens, single-source (2L1S) microlensing event is an astronomical phenomenon where the light from a distant source star is bent and magnified as it passes through a binary star system. This phenomenon offers a unique opportunity to study and discover exoplanets. Fast and automated inference of 2L1S microlensing events using MCMC methods faces two main challenges: (a) the high computational cost of likelihood evaluations using microlensing simulation codes, and (b) the complexity parameter space characterized by a negative-log-likelihood surface riddled with numerous narrow and deep local minima.

This section examines the 2L1S microlensing model explored in [Zhang et al. \(2021\)](#). In our analysis, we fix the angle of the source trajectory relative to the projected binary lens axis at  $\alpha = 110$  degrees and the time of closest approach at  $t_0 = 60.0$  day. The model comprises five unknown parameters in the model: binary lens separation ( $s$ ), mass ratio ( $q$ ), impact parameter ( $u_0$ ), Einstein ring crossing timescale ( $t_E$ ), and source flux fraction ( $f_s$ ).

We simulate the 2L1S magnification sequences using the microlensing code *MulensModel* ([Poleski and Yee, 2019](#)) over a 144 days period with a cadence of 15 minutes, resulting in  $N_{\mathbf{y}} = 13825$  observations. The observed data  $\mathbf{y}$  is generated using the parameters  $(s, q, u_0, t_E, f_s) = (10^{-0.2}, 10^{-2.5}, 0.2, 10^{1.6}, 0.2)$ . The discrepancy between the observed data  $\mathbf{y}$  and the simulated data  $\mathbf{x}$  is defined as  $\Delta(\mathbf{x}, \mathbf{y}) = \frac{1}{N_{\mathbf{y}}} \sum_{i=1}^{N_{\mathbf{y}}} |\mathbf{y}_i - \mathbf{x}_i|$ . A Gaussian kernel with a bandwidth  $\varepsilon = 0.003$  is employed. We simulate 2L1S events using the analytical priors:  $s \sim \text{LogUniform}(0.2, 0.5)$ ,  $q \sim \text{LogUniform}(10^{-6}, 1)$ ,  $u_0 \sim \text{Uniform}(0, 2)$ ,  $t_E \sim \text{TruncLogNorm}(1, 100, \mu = 10^{1.15}, \sigma = 10^{0.45})$ , and  $f_s \sim \text{LogUniform}(0.1, 1)$ .

For local proposals, we use the following distributions:  $\log(s^*) \sim N(\log(s), 0.2^2)$ ,  $\log(q^*) \sim N(\log(q), 0.2^2)$ ,  $u_0^* \sim N(u_0, 0.01^2)$ ,  $\log(t_E^*) \sim N(\log(t_E), 0.05^2)$ , and  $\log(f_s^*) \sim N(\log(f_s), 0.05^2)$ . Due to the model's complexity, we derive the importance proposal from a coarse posterior estimate obtained by running 5,000 iterations of simple rejection sampling with a large threshold of  $\varepsilon = 0.05$ .

Considering simulation costs, a sequential optimization algorithm is employed to determine the global frequency  $\gamma$  and the batch size  $N_b$ , constrained by  $\gamma N_b + (1 - \gamma) = C$ , to maintain the average number of simulation per iteration to  $C = 3$ . For each potential set of hyperparameters,

we perform GL-ABC-MCMC with 5,000 iterations, repeating this process five times.

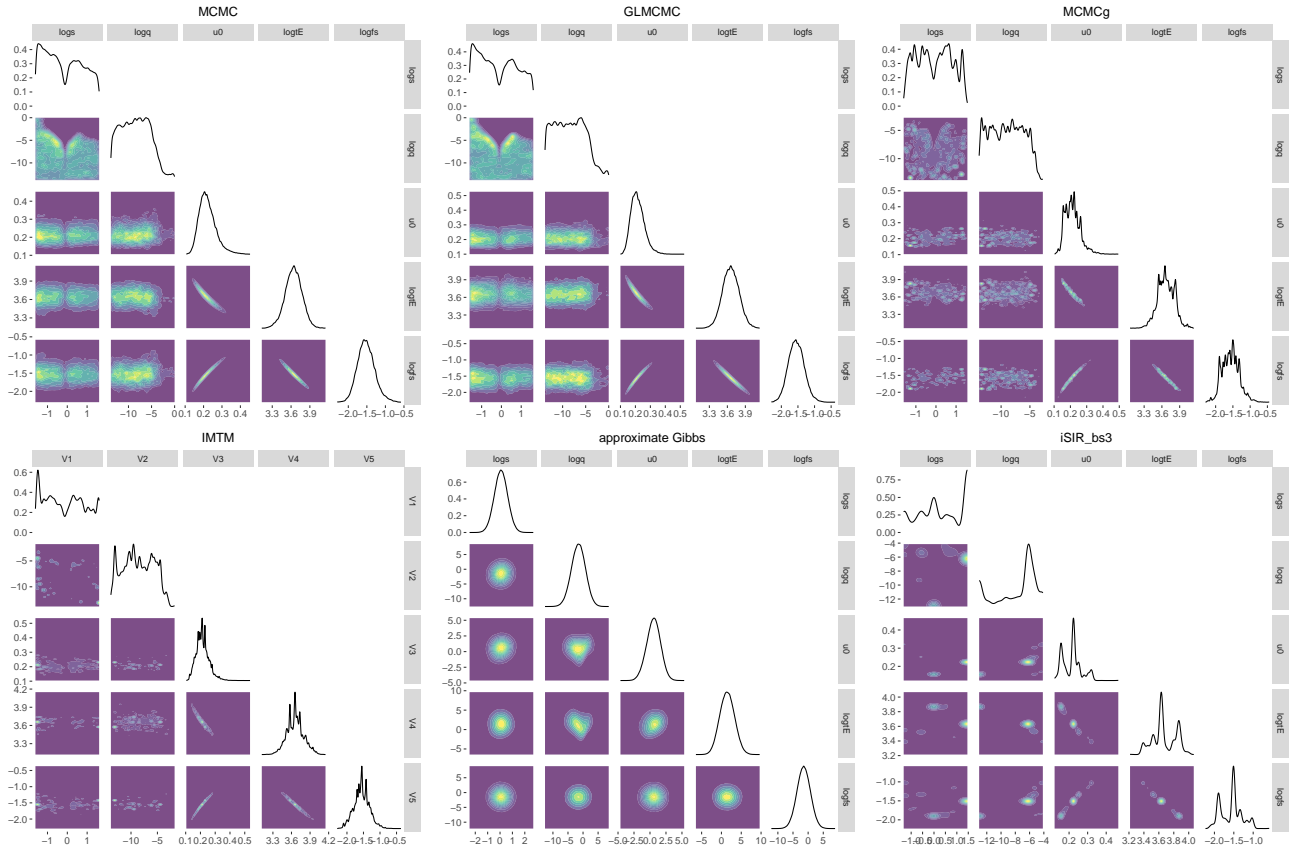


Figure 6: Visualization of the posterior distributions estimated by various ABC-MCMC methods.

Figure 6 presents the posterior estimates obtained via basic ABC-MCMC with a random walk proposal, ABC-MCMC with the importance proposal as the global proposal (MCMCg), GL-ABC-MCMC, ABC-iSIR with batch size 3, independent multiple try Metropolis (IMTM) (Martino, 2018) and the likelihood-free approximate Gibbs (Rodrigues et al., 2020). The basic ABC-MCMC, MCMCg and GL-ABC-MCMC are all executed over 500,000 iterations. We use a Gaussian process model to approximate the full conditional distributions, and 50,000 train data is from importance proposal. We run the approximate Gibbs 110,000 iterations and discard the first 10,000 iterations as burn-in. Firstly, ABC-MCMC with global proposal, ABC-iSIR and independent multiple try Metropolis (IMTM) with batch-size 3 present random walk behavior, and the approximate Gibbs fails to capture the multiple modes of the posterior distribution. Both the standard ABC-MCMC and GL-ABC-MCMC can effectively explore both peaks of the posterior. Subsequently, we compare the effective sample size (ESS) of GL-ABC-MCMC against that of tra-

ditional ABC-MCMC approaches. ABC-MCMC<sub>1</sub> is configured with the same number of iterations as GL-ABC-MCMC, while ABC-MCMC<sub>2</sub> is adjusted to have a comparable number of simulations as GL-ABC-MCMC. According to Table 2, GL-ABC-MCMC demonstrates a significantly larger ESS compared to both ABC-MCMC<sub>1</sub> and ABC-MCMC<sub>2</sub>, indicating superior performance of our GL-ABC-MCMC approach. Table 3 shows the estimates of the posterior mean and credible intervals for different methods. The posterior mean obtained from GL-ABC-MCMC is closer to the true value, and the GL-ABC-MCMC estimate exhibits a narrower 95% credible interval.

Table 2: Comparison of effective sample sizes of different methods. ABC-MCMC<sub>1</sub>:  $N = 500,000$ ; ABC-MCMC<sub>2</sub>:  $N = 1,500,000$ ; GL-ABC-MCMC:  $N = 500,000$  and the average number of simulations per iteration is 3.

Method	$\log(s)$	$\log(q)$	$u_0$	$\log(t_E)$	$\log(f_s)$
ABC-MCMC <sub>1</sub>	579.84	75.10	356.57	405.17	382.94
ABC-MCMC <sub>2</sub>	<b>1768.85</b>	229.93	973.57	1096.42	1019.30
GL-ABC-MCMC	1389.22	<b>748.04</b>	<b>2235.37</b>	<b>2270.99</b>	<b>2172.30</b>

Table 3: Comparison of posterior mean and 95% credible intervals of different methods.

Method	$\log(s)$	$\log(q)$	$u_0$	$\log(t_E)$	$\log(f_s)$
Ture	-0.4605	-5.7565	0.2	3.6841	-1.6094
ABC-MCMC <sub>1</sub>	-0.1716 (-1.55,1.49)	-8.4197 (-13.49,-2.39)	0.2215 (0.15,0.33)	3.6402 (3.37,3.90)	-1.5183 (-1.94,-1.01)
ABC-MCMC <sub>2</sub>	<b>-0.1079</b> (-1.55,1.51)	-8.4456 (-13.51,-2.79)	0.2240 (0.15,0.34)	3.6349 (3.36,3.91)	-1.5082 (-1.97,-0.99)
GL-ABC-MCMC	-0.1657 (-1.56,1.50)	<b>-8.3515</b> (-13.57,-1.76)	<b>0.2158</b> (0.14,0.32)	<b>3.6577</b> (3.39,3.93)	<b>-1.5500</b> (-2.00,-1.07)

## 5.2 Example 2: A stochastic differential equation example

We consider parameter estimation of a high dimensional non-linear example, the Van der Pol oscillator model (Kandepu et al., 2008; Särkkä et al., 2015). The model is described by the

following second-order non-linear ODE:

$$\frac{d^2x(t)}{dt^2} - \mu(1 - \epsilon x^2(t))\frac{dx(t)}{dt} + x(t) = f(t).$$

The unknown parameters in the model are  $\mu$  and  $\epsilon$ , and  $f(t)$  represents an additional unknown forcing term. To model the forcing term  $f(t)$ , we assume it is a combination of white noise and a stochastic resonator  $c(t)$ , which is formed by the sum of  $N$  harmonic components  $c_n(t)$ :

$$\frac{d^2c_n(t)}{dt^2} = -(n\omega_c)^2c_n(t) + \sigma_n\epsilon_n(t).$$

Here  $\omega_c$  represents the angular velocity of the force process,  $\sigma_n$  represents the strength of the noise process driving the  $n$ th harmonic, and  $\epsilon_n(t)$  represents a white noise process. In this section, we set  $N = 2$ . For simplicity, we assume that  $\sigma_n = \sigma_c$  for all  $n = 1, 2$ . Consequently, the parameter vector  $\boldsymbol{\theta} = (\epsilon, \mu, \sigma, \omega_c, \sigma_c)$  is five-dimensional, and the state variable  $\mathbf{x} = (x, \dot{x}, c_1, \dot{c}_1, c_2, \dot{c}_2)$  has 6 components. The full SDE model can be represented as:

$$\begin{aligned} dx(t) &= \dot{x}(t)dt, \\ d\dot{x}(t) &= \mu(1 - \epsilon x^2(t))\dot{x}(t)dt - x(t)dt + (c_1(t) + c_2(t))dt, \\ dc_n(t) &= \dot{c}_n(t)dt, \\ d\dot{c}_n(t) &= -(\omega_c)^2c_n(t)dt + \sigma_c dW_n(t), \quad \text{for } n = 1, 2. \end{aligned}$$

Here,  $dW_n(t)$  represents the differential of a standard Wiener process. The measurements are obtained by adding noise to the state of the Van der Pol oscillator:

$$y_k = x(t_k) + r_k, \quad r_k \sim \mathcal{N}(0, \sigma^2).$$

The observed data  $\mathbf{y}$  was simulated from the system using the parameter values  $\boldsymbol{\theta} = (1, 1/2, 1/10, \pi/5, 1/100)$  over the time interval  $t \in [0, 40]$ , with a sampling period of  $\Delta t = 1$ . Since  $\boldsymbol{\theta} \geq 0$ , we take Gamma distributions as prior distributions  $\pi(\boldsymbol{\theta})$ :  $\epsilon \sim \text{Gamma}(5, 1)$ ,  $\mu \sim \text{Gamma}(3, 5)$ ,  $\sigma \sim \text{Gamma}(5, 15)$ ,  $\omega_c \sim \text{Gamma}(5, 10)$ ,  $\sigma_c \sim \text{Gamma}(2, 15)$ . Here, we choose the kernel function  $K_\epsilon(\cdot, \mathbf{y}) = N(\cdot; \mathbf{y}, \epsilon^2)$  with an ABC threshold  $\epsilon = 0.15$ .

We obtain the true posterior by running 5 ABC-MCMC chains with 1,000,000 iterations, and discard the first 50,000 iterations as the burn-in. We use “density” function in  $R$  to estimate the 1D marginal density with 512 points on the posterior region, specifically is  $[0, 12] \times [0, 1.5] \times [0, 1] \times$



$[0, 1.5] \times [0, 0.5]$ . The KL divergence is calculated as follows:

$$D_{KL}(\pi_\varepsilon(\theta_i) \mid \hat{\pi}_\varepsilon(\theta_i)) = \frac{l_i}{|\Theta_{i,ref}|} \sum_{\theta_i \in \Theta_{i,ref}} \pi_\varepsilon(\theta_i \mid \mathbf{y}) \log \frac{\pi_\varepsilon(\theta_i \mid \mathbf{y})}{\hat{\pi}_\varepsilon(\theta_i \mid \mathbf{y})},$$

where  $\pi_\varepsilon(\theta_i)$  is the true ABC posterior marginal density of  $\theta_i$ ,  $\hat{\pi}_\varepsilon(\theta_i)$  is the estimated ABC posterior marginal density of  $\theta_i$ , and  $l_i$  is the length of the interval for the posterior estimate. Here, we examine the robustness of our sequential optimization algorithm for selecting  $\gamma$  by implementing GL-ABC-MCMC with two different ABC-i-SIR proposal distributions. The batch size of ABC-i-SIR is set to  $N_b = 20$ . In the first scenario, we use the prior distribution as the importance proposal, denoted as GLMCMC<sub>1</sub>. In the second scenario, we use a flatter density as the proposal distribution, denoted as GLMCMC<sub>2</sub>. We use cESJD to select the global frequency  $\gamma$ . The detailed setups and results are shown in Supplementary S.3.4. We select  $\gamma = 1$  for GLMCMC<sub>1</sub> and  $\gamma = 0.8$  for GLMCMC<sub>2</sub> based on the cESJD. The result implies that the global move of GLMCMC<sub>1</sub> performs sufficiently well, whereas GLMCMC<sub>2</sub> requires a combination of global and local moves to maximize the efficiency of the algorithm. The proportion of global moves of GLMCMC<sub>1</sub> is higher than GLMCMC<sub>2</sub> since the importance proposal of GLMCMC<sub>1</sub> is closer to the target compared with the GLMCMC<sub>2</sub>. The result also indicates the effectiveness of the cESJD criterion and the robustness of the GL-ABC-MCMC algorithm with respect to the hyperparameter  $\gamma$ .

We compute the KL divergence of different methods at iteration numbers  $10^5$ ,  $2 \cdot 10^5$ , ...,  $10^6$ . We take the time executing one MCMC iteration as the baseline. Figure 7 shows the KL divergence of different methods varying with time cost. The methods proposed in this article (*i.e.*, GL-ABC-MCMC) converge faster than ordinary MCMC, and admit smaller variance. The pairwise marginals of the parameters are shown in Supplementary S.3.4, Figure S.5.

## 6 Conclusion

In this article, we consider the task of Bayesian inference for models with intractable likelihood function. Markov chain Monte Carlo methods are often combined with ABC to accelerate the likelihood-free inference. MCMC with local moves often struggles to explore posterior distribution with complex surface. Hence, we design efficient global and local moves to explore the challenge posterior surfaces in the likelihood-free framework.

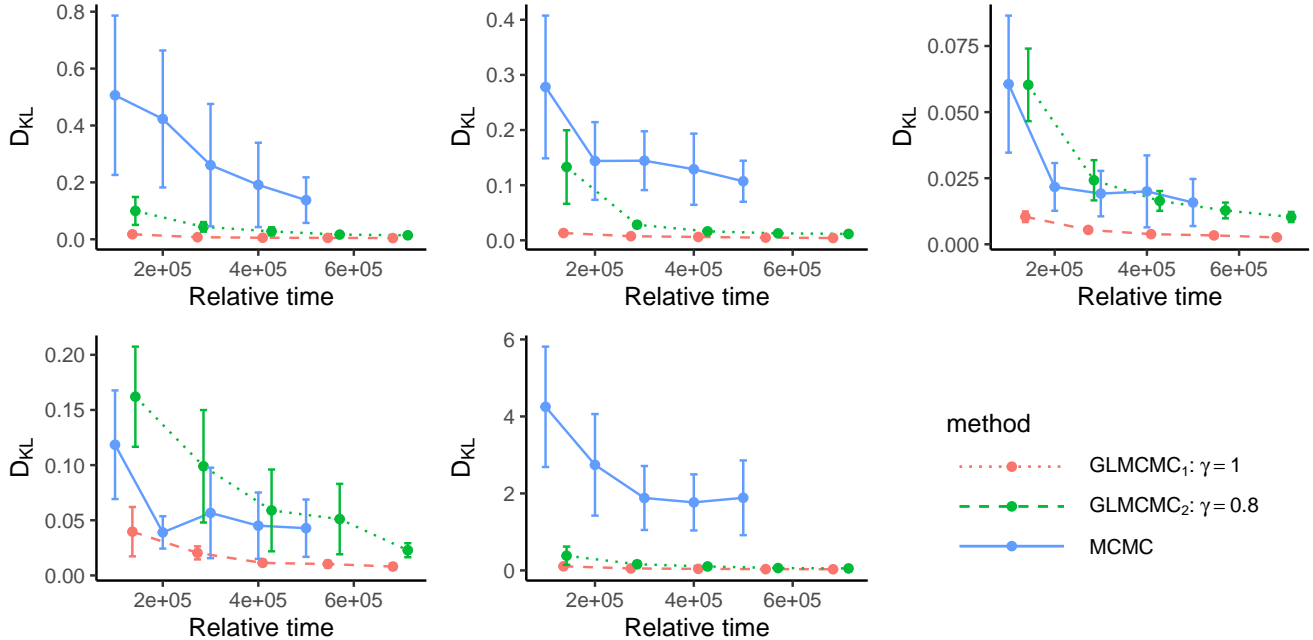


Figure 7: Comparison of three ABC-MCMC methods (ABC-MCMC, ABC-i-SIR with batch size 20, and GL-ABC-MCMC with batch size 20 and global frequency 0.1 and 0.3). Error bars denote 95% confidence intervals for  $D_{KL}$  across 10 replicates. First row:  $\epsilon$ ,  $\mu$ ,  $\sigma$ ; Second row:  $\omega_c$ ,  $\sigma_c$ .

A likelihood free version of i-SIR is developed to serve as global proposals of ABC-MCMC algorithms, and we propose using sequential optimization algorithm to select the hyper-parameters based on a unit cost version of ESJD. We also prove the V-geometric ergodicity of the ABC Global-Local Markov kernel, which indicates that under certain conditions, the mixing rate of the proposed Markov Kernel is significantly better than the corresponding mixing rate of the local kernel.

Two adaptive schemes are designed to improve the efficiency of our proposed ABC-MCMC. In our first adaptive scheme, we incorporate normalizing flow into ABC-i-SIR to train the proposal distribution. In the second adaptive scheme, we design an ABC version of MALA algorithm, in which the gradient of log-likelihood function is evaluated using the common random numbers technique. Numerical experiments demonstrate that our algorithm outperforms existing methods in synthetic and real application models.

There are several lines of extensions and improvements for future work. The ABC tolerance  $\epsilon$  is pre-specified before running our ABC-MCMC. [Del Moral et al. \(2012\)](#) provide a framework

for adaptively selecting the sequence of tolerance for ABC within the sequential Monte Carlo (SMC). Our first line of future work is to combine our Global-Local moves with ABC-SMC and investigate adaptive schemes to tune the parameters in the moves. The computation of MH acceptance probability  $\alpha$  involves generating synthetic data from the simulation model, which may cause a heavy computational burden for complex problems. Our second line of future work is to accelerate the ABC-MCMC inference speed by using approximations (*e.g.* [Cao et al. \(2024\)](#); [Rodrigues et al. \(2020\)](#)). A large number of simulations are required to evaluate the gradient function of approximate Bayesian methods for high-dimensional parameter spaces. Our third line of future research is to generate control variates for variance reduction and determine the optimal simulation size for gradient approximation.

## Supplementary Materials

**S.1:** Some details of algorithms not shown in the main text.

**S.2:** The proofs of all theoretical results presented in the main text.

**S.3:** Some numerical results and some details of setups not shown in the main text.

## Acknowledgements

This work was supported by the National Natural Science Foundation of China (12131001 and 12101333), the startup fund of ShanghaiTech University, the Fundamental Research Funds for the Central Universities, LPMC, and KLMDASR. The authorship is listed in alphabetic order.

## References

- Andrieu, C., A. Doucet, and R. Holenstein (2010). Particle markov chain monte carlo methods. *Journal of the Royal Statistical Society Series B: Statistical Methodology* 72(3), 269–342.
- Andrieu, C., A. Lee, and M. Vihola (2018). Uniform ergodicity of the iterated conditional smc and geometric ergodicity of particle gibbs samplers. *Bernoulli* 24(2), 842–872.

- Atchadé, Y. F., G. O. Roberts, and J. S. Rosenthal (2011). Towards optimal scaling of metropolis-coupled markov chain monte carlo. *Statistics and Computing* 21, 555–568.
- Beaumont, M. A., W. Zhang, and D. J. Balding (2002, 12). Approximate Bayesian computation in population genetics. *Genetics* 162(4), 2025–2035.
- Cao, X., S. Wang, and Y. Zhou (2024). Using early rejection markov chain monte carlo and gaussian processes to accelerate abc methods. *Journal of Computational and Graphical Statistics* 0(0), 1–14.
- Clarté, G., C. P. Robert, R. J. Ryder, and J. Stoehr (2020, 11). Componentwise approximate Bayesian computation via Gibbs-like steps. *Biometrika* 108(3), 591–607.
- Del Moral, P., A. Doucet, and A. Jasra (2006). Sequential Monte Carlo samplers. *Journal of the Royal Statistical Society: Series B (Statistical Methodology)* 68(3), 411–436.
- Del Moral, P., A. Doucet, and A. Jasra (2012). An adaptive sequential Monte Carlo method for approximate Bayesian computation. *Statistics and Computing* 22(5), 1009–1020.
- Duane, S., A. Kennedy, B. J. Pendleton, and D. Roweth (1987). Hybrid monte carlo. *Physics Letters B* 195(2), 216–222.
- Fang, K.-T., M.-Q. Liu, H. Qin, and R. Zhang (2018). *Theory and Application of Uniform Experimental Designs*. Singapore: Springer.
- Gabriel, M., G. M. Rotskoff, and E. Vanden-Eijnden (2022). Adaptive monte carlo augmented with normalizing flows. *Proceedings of the National Academy of Sciences* 119(10), e2109420119.
- Girolami, M. and B. Calderhead (2011). Riemann manifold langevin and hamiltonian monte carlo methods. *Journal of the Royal Statistical Society Series B: Statistical Methodology* 73(2), 123–214.
- Grenander, U. and M. I. Miller (1994). Representations of knowledge in complex systems. *Journal of the Royal Statistical Society. Series B (Methodological)* 56(4), 549–603.
- Kandepu, R., B. Foss, and L. Imsland (2008). Applying the unscented kalman filter for nonlinear state estimation. *Journal of process control* 18(7-8), 753–768.
- Marjoram, P., J. Molitor, V. Plagnol, and S. Tavaré (2003). Markov chain Monte Carlo without likelihoods. *Proceedings of the National Academy of Sciences* 100(26), 15324–15328.
- Martino, L. (2018). A review of multiple try mcmc algorithms for signal processing. *Digital Signal Processing* 75, 134–152.
- Meeds, E., R. Leenders, and M. Welling (2015). Hamiltonian abc. *arXiv preprint arXiv:1503.01916*.
- Neal, R. M. et al. (2011). Mcmc using hamiltonian dynamics. *Handbook of markov chain monte carlo* 2(11), 2.
- Papamakarios, G., E. Nalisnick, D. J. Rezende, S. Mohamed, and B. Lakshminarayanan (2021). Normalizing flows for probabilistic modeling and inference. *The Journal of Machine Learning Research* 22(1), 2617–2680.

- Parno, M. D. and Y. M. Marzouk (2018). Transport map accelerated markov chain monte carlo. *SIAM/ASA Journal on Uncertainty Quantification* 6(2), 645–682.
- Pasarica, C. and A. Gelman (2010). Adaptively scaling the metropolis algorithm using expected squared jumped distance. *Statistica Sinica*, 343–364.
- Poleski, R. and J. C. Yee (2019). Modeling microlensing events with mulensmodel. *Astronomy and computing* 26, 35–49.
- Pritchard, J. K., M. T. Seielstad, A. Perez-Lezaun, and M. W. Feldman (1999, 12). Population growth of human Y chromosomes: a study of Y chromosome microsatellites. *Molecular Biology and Evolution* 16(12), 1791–1798.
- Rezende, D. and S. Mohamed (2015). Variational inference with normalizing flows. In *International conference on machine learning*, pp. 1530–1538. PMLR.
- Roberts, G. and J. Rosenthal (2014). Minimising mcmc variance via diffusion limits, with an application to simulated tempering. *Annals of Applied Probability* 24(1), 131–149.
- Roberts, G. O. and J. S. Rosenthal (1998). Optimal scaling of discrete approximations to langevin diffusions. *Journal of the Royal Statistical Society: Series B (Statistical Methodology)* 60(1), 255–268.
- Roberts, G. O. and R. L. Tweedie (1996). Exponential convergence of langevin distributions and their discrete approximations. *Bernoulli*, 341–363.
- Rodrigues, G. S., D. J. Nott, and S. A. Sisson (2020). Likelihood-free approximate gibbs sampling. *Statistics and Computing* 30(4), 1057–1073.
- Samsonov, S., E. Lagutin, M. Gabrié, A. Durmus, A. Naumov, and E. Moulines (2022). Local-global mcmc kernels: the best of both worlds. *Advances in Neural Information Processing Systems* 35, 5178–5193.
- Särkkä, S., J. Hartikainen, I. S. Mbalawata, and H. Haario (2015). Posterior inference on parameters of stochastic differential equations via non-linear gaussian filtering and adaptive mcmc. *Statistics and Computing* 25(2), 427–437.
- Sisson, S. A., Y. Fan, and M. M. Tanaka (2007). Sequential Monte Carlo without likelihoods. *Proceedings of the National Academy of Sciences* 104(6), 1760–1765.
- Tavaré, S., D. J. Balding, R. C. Griffiths, and P. Donnelly (1997). Inferring coalescence times from dna sequence data. *Genetics* 145(2), 505–518.
- Tjelmeland, H. (2004). Using all metropolis–hastings proposals to estimate mean values. Technical report.
- Wand, M. P. (1994). Fast computation of multivariate kernel estimators. *Journal of Computational and Graphical Statistics* 3(4), 433–445.
- Wegmann, D., C. Leuenberger, and L. Excoffier (2009, 08). Efficient approximate Bayesian computation coupled with Markov chain Monte Carlo without likelihood. *Genetics* 182(4), 1207–1218.

- Yang, J., G. O. Roberts, and J. S. Rosenthal (2020). Optimal scaling of random-walk metropolis algorithms on general target distributions. *Stochastic Processes and their Applications* 130(10), 6094–6132.
- Yang, Z. and A. Zhang (2021). Hyperparameter optimization via sequential uniform designs. *Journal of Machine Learning Research* 22(149), 1–47.
- Zhang, K., J. S. Bloom, B. S. Gaudi, F. Lanusse, C. Lam, and J. R. Lu (2021). Real-time likelihood-free inference of roman binary microlensing events with amortized neural posterior estimation. *The Astronomical Journal* 161(6), 262.